# Planar Fe$_6$ Cluster Units in the Crystal Structure of RE$_{15}$Fe$_8$C$_{25}$ (RE = Y, Dy, Ho, Er)**

*Bambar Davaasuren, Horst Borrmann, Enkhtsetseg Dashjav, Guido Kreiner, Michael Widom, Walter Schnelle, Frank R. Wagner, and Rüdiger Kniep\**

Carbometalates represent a special class of ternary and higher carbides containing complex anions $^n_\infty[(T_yC_z)^{m-}]$ ($n = 0, 1, 2, 3$) characterized by covalent bonds between the transition metals (T) and the highly polarizable (monoatomic) carbon species.[1] The negative charge of the carbo ligands (C$^{4-}$) together with the low oxidation states of the transition metals cause high negative charges on the complex carbometalate anions, which have to be balanced by cations bearing a high positive charge, as brought about by rare-earth elements (RE), and resulting in the general formula RE$_x$[T$_y$C$_z$]. Carbometalates as electron-precise compounds without a tendency to form perceptible homogeneity ranges and exclusively containing monoatomic carbo ligands are shown to exist in a range of atomic ratios given by the condition ($x + y$)/$z \leq 2$.[1] In the systems REFeC, several ternary phases fulfilling this compositional condition have been reported. However, their crystal structures either contain C$_2$ pairs as structural units instead of monoatomic carbo ligands, such as RE$_2$[Fe(C$_2$)$_{4/2}$] (RE = Y, Tb–Lu),[2] Sc$_3$[Fe(C$_2$)$_{4/2}$],[3,4] RE-[FeC$_2$] (RE = Sc, Sm, Gd–Er, Lu),[5,6] and RE$_{3.67}$[Fe(C$_2$)$_3$] (RE = La–Nd, Sm)[7,8]), or the crystal structures have not been determined (GdFeC, RE$_2$Fe$_2$C$_3$, RE$_4$Fe$_4$C$_7$ (RE = Ce, Gd)).[9,10] Our continuous search for carboferrates exclusively containing monoatomic carbo ligands has been unsuccessful so far. Instead, we obtained a new series of isotypic compounds, RE$_{15}$Fe$_8$C$_{25}$ (RE = Y, Dy, Ho, Er), containing the novel structural unit of a Fe$_6$ cluster surrounded by C$_2$ pairs and a monoatomic carbon species. Crystal structure and materials properties as well as the chemical bonding situation in these compounds are discussed in detail.

The metallic-gray rare-earth iron carbides were prepared by a high-temperature route,[11] and their crystal structures

[*] B. Davaasuren, Dr. H. Borrmann, Dr. E. Dashjav, Dr. G. Kreiner, Dr. W. Schnelle, Dr. F. R. Wagner, Prof. Dr. R. Kniep
Max-Planck-Institut für Chemische Physik fester Stoffe
Nöthnitzer Strasse 40, 01187 Dresden (Germany)
Fax: (+ 49) 351-4646-3002
E-mail: kniep@cpfs.mpg.de

Prof. Dr. M. Widom
Department of Physics, Carnegie Mellon University
Pittsburgh, PA 15213 (USA)

Supporting information for this article is available on the WWW under http://dx.doi.org/10.1002/anie.201002338.

were determined from X-ray diffraction data (single crystals as well as powders).[12,13] The crystal structure is exemplarily described for the Er compound.

The striking feature of the crystal structure is an unusual planar group of six Fe atoms, which are arranged to form a triangle with Fe atoms at the vertices (Fe1) and at the midpoints of the edges (Fe2) as shown in Figure 1. The
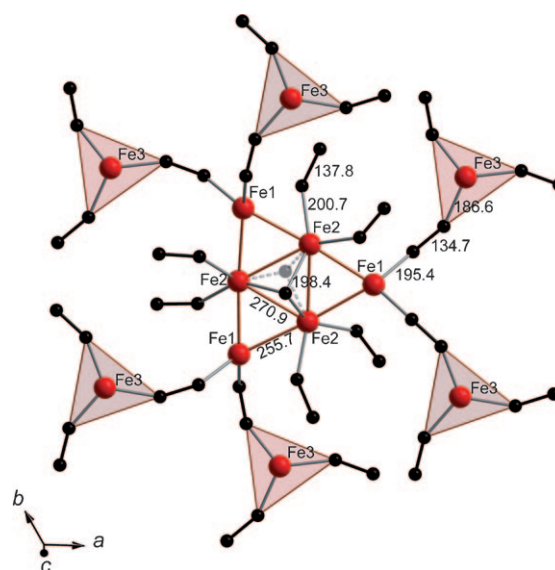


**Figure 1.** Planar Fe$_6$ cluster in the crystal structure of Er$_{15}$Fe$_8$C$_{25}$ surrounded by 12 C$_2$ pairs, 6 of which are also part of trigonal planar [Fe(C$_2$)$_3$] units. A monoatomic carbon ligand takes a position either above or below the Fe2 triangle.

triangle can be regarded as fragments of the crystal structures of $\gamma$-Fe,[14] $\varepsilon$-Fe$_3$C,[15] and $\eta$-Fe$_2$C.[16] The short Fe–Fe distances in the ternary phase (Fe1–Fe2 = 255.7(1) pm and Fe2–Fe2 = 270.9(1) pm) fall between the respective distances in $\gamma$-Fe (242.5 pm), $\varepsilon$-Fe$_3$C (275.4 pm), and $\eta$-Fe$_2$C (260.6 pm and 277.8 pm).

The Fe$_6$ cluster is surrounded by one monoatomic carbon ligand (either above or below the small Fe2 triangle) and 12 carbon pairs bonded non-coplanar end on to the iron atoms of the cluster. Considering the coordination of iron atoms of the Fe$_6$ triangles by carbon ligands only, distorted Fe1(C$_2$)$_4$ tetrahedra and trigonal pyramids Fe2C(C$_2$)$_2$ resemble the structural motifs commonly found in the crystal structures of carbometalates.[1,17] By taking into consideration also the short Fe–Fe contacts, the coordination polyhedra around Fe1 and Fe2 can be considered as strongly distorted octahedra

(4 C + 2 Fe) and polyhedra formed by seven corners (3 C + 4 Fe), respectively. Fe3 atoms in the crystal structure serve as linkers between the $Fe_6$ clusters. Interlinking is realized by bonding (end-on) of three $C_2$-pairs (C−C 134.7(3) pm) to Fe3 (Fe−C 186.6(2) pm) and formation of a trigonal-planar arrangement. The $C_2$ units bonded to Fe2 (C−C 137.8(3) pm, Fe−C 200.7(2) pm) do not participate in further linkages within the complex anion. The $Fe_6$ clusters are connected to six neighboring clusters through six planar $Fe3(C_2)_3$ groups resulting in overall, infinite layers $_\infty^2[(Fe_6)Fe_2(C_2)_{12}C]$. Because of the space-consuming ligands surrounding the clusters, and their linking through isolated structural units, the distance between neighboring clusters within a layer becomes very large (1186 pm between the centers of the clusters).

The layers $_\infty^2[(Fe_6)Fe_2(C_2)_{12}C]$ are stacked along [001] as shown in Figure 2a. Together with the presentation in Fig-
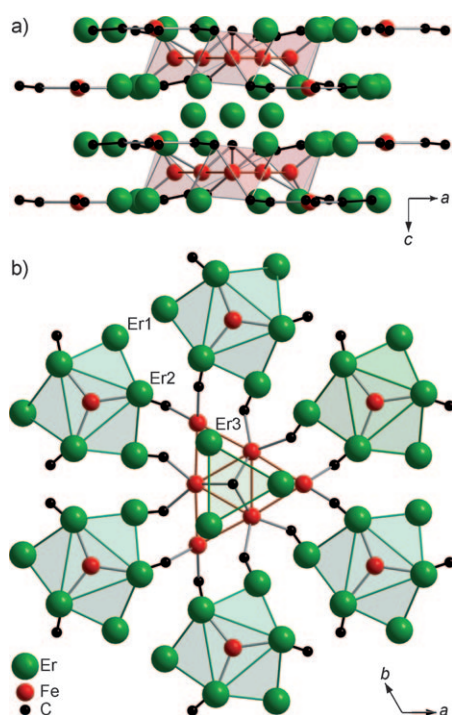


*Figure 2.* a) Stacking of layers in the crystal structure of $Er_{15}Fe_8C_{25}$ viewed along the [010] direction. b) Crystal structure viewed along the [001] direction. See text for further details.

ure 2b, it becomes clear that Er3 atoms are sandwiched between the $Fe_6$ clusters of adjacent layers. The remaining Er atoms (Er1 and Er2) form tricapped trigonal-prismatic arrangements surrounding the $Fe3(C_2)_3$ units. These tricapped trigonal prisms form columns running along [001] by sharing common basal planes. The columns are arranged to form a honeycomb pattern with the $Fe_6$ clusters (capped with additional Er3 atoms above and below the cluster plane) taking positions inside the large channels.

For charge balancing, simple rules of electron counting based on ionic concepts can be used with the following strategy: the polymeric complex anion $_\infty^2[(Fe_6)Fe_2(C_2)_{12}C]$

bears a total charge of 45− by counting the RE species (in agreement with susceptibility data; see below) as $RE^{3+}$ (resulting in $RE_{15} = 45 +$). Further assumptions concern the charges of the mono- and diatomic carbon ligands based on the crystal-chemical concept of carbometalates[1] as well as on experimental values of C−C distances in $C_2$ pairs.[2–10] For the present compounds, these data allow one to count the monoatomic carbon as $C^{4-}$, and the diatomic species as $C_2^{4-}$. The iron clusters (Fe1, Fe2) in the crystal structure are interconnected by Fe3 in a trigonal-planar coordination arrangement by $C_2$ pairs. Trigonal-planar $[Fe(C_2)_3]$ groups are also known from the crystal structure of $RE_{3.67}[Fe(C_2)_3]$[7,8] with the Fe atoms being assigned to the valence state of $Fe^{1+}$. Altogether, the (ionic) chemical formula of the cluster compounds can be written as $(RE^{3+})_{15}[(Fe_6)^{5+}(Fe^{1+})_2 - (C_2^{4-})_{12}C^{4-}]$, resulting in a mean valence state of the six iron atoms of the cluster unit of 0.83 +, which, in general, would be consistent with homoatomic bonding interactions within the clusters.

The corrected magnetic susceptibilities $\chi_{corr}(T)$ of $RE_{15}Fe_8C_{25}$ (RE = Dy, Ho, Er) are in accordance with the presence of strongly paramagnetic $RE^{3+}$ ions ($\mu_{eff} = 38$–41 $\mu_B$ f.u.$^{-1}$; f.u.: formula unit; see the Supporting Information). A discussion of the physical properties and calculations concerning the chemical bonding situation is given below for the Y compound. The temperature dependence of the corrected susceptibility $\chi_{corr}$ of $Y_{15}Fe_8C_{25}$ resembles a Curie–Weiss law and a fit results in a weak paramagnetic moment $\mu_{eff} = 6 \pm 1$ $\mu_B$ f.u.$^{-1}$ A broad shoulder visible at around 30 K in $\chi_{corr}(T)$ might be interpreted as a ferromagnetic ordering transition. In this case, the ordered moment would be $\mu_{ord} \approx 0.8$ $\mu_B$ f.u.$^{-1}$ The electrical resistivity $\rho(T)$ measured on compact pieces shows a metallike temperature dependence above 50 K ($\rho(300 K) = 330$ $\mu\Omega$ cm). The curve $\rho(T)$ shows a minimum around 38 K followed by a slight increase (+7%) towards 4 K. The origin of this behavior remains unexplained, although the temperature of the minimum in $\rho(T)$ coincides with the shoulder in $\chi_{corr}$. Both features might indicate a magnetic ordering of the Fe units.

DFT/PW91[18] total-energy calculations on $Y_{15}Fe_8C_{25}$ reveal that magnetic phases with an ordered moment of about 6 $\mu_B$ f.u.$^{-1}$ are energetically favorable, lowering the total energy of the magnetic phase by about 0.2 eV f.u.$^{-1}$ with respect to the nonmagnetic one (see the Supporting Information). The results further indicate the presence of one-sided location of the monoatomic carbon atom above or below the $Fe_6$ plane.

Electronic band structure calculations using the TB-LMTO-ASA method[19] within the local density approximation[20] reveals metallic character, which generally agrees with the resistivity measurements. The spin-polarized calculation with ferromagnetic ordering yields a total magnetic moment of about 5 $\mu_B$ f.u.$^{-1}$, which is consistent with the magnetic moments obtained from total energy calculations. The density-of-states (DOS) curves of the minority and majority spin channels are rather similar (see the Supporting Information). The total DOS (Figure 3a) displays a characteristic structuring into separated parts from nominal diatomic ($\sigma_s$: *A1*, $\sigma^*_s$: *A2*) and monoatomic carbon species (C(2s): *B*), as
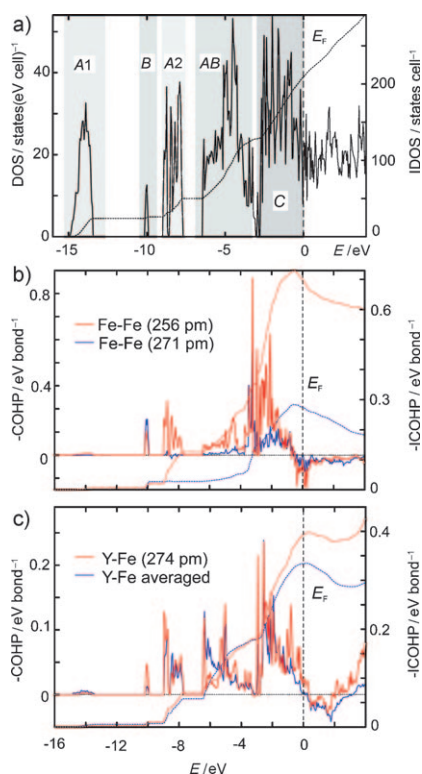
**Figure 3.** a) Total DOS with regions *A1*, *B*, *A2*, *AB*, and *C* (see text) and b,c) spin-averaged COHP diagrams for interatomic interactions Fe–Fe and Fe–Y of $Y_{15}Fe_8C_{25}$.

well as a common region of C(2p) states (*AB*), and a mainly metal-dominated part (*C*) starting below the Fermi level $E_F$ and extending further on, similar to that found for $La_7Os_4C_9$.[21]

Complementary chemical bonding analysis with a focus on metal–metal interactions was performed employing the COHP (crystal orbital Hamiltonian population) method[22], as well as the electron localizability indicator (ELI-D),[23] and the QTAIM (quantum theory of atoms in molecules) method.[24] The COHP diagram (Figure 3b) shows that some Fe–Fe bonding orbital interactions already start to develop for the nominal carbon DOS parts. The maximum number of bonding interactions, however, is achieved within the nominal metal bands in the uppermost part of the DOS. Notably, all the bonding states are exhausted below $E_F$, but at $E_F$ a small number of antibonding states are already occupied continuing further beyond. Almost the same situation is observed (Figure 3c) for the Fe–Y interactions with the slight difference that $E_F$ more clearly marks the boundary between all occupied bonding and all empty antibonding interactions. For $Y_{15}Fe_8C_{25}$, the ratios of ICOHP(metal–C)/ICOHP(metal–metal) ≈ 3 and ICOHP(Fe–C) ≫ ICOHP(Y–C) are within the range of values observed for carbometalates.[1]

Further aspects of metal–metal bonding can be extracted from topological analysis of the ELI-D and the electron density. The $Fe_6$ cluster bonding is characterized by a number of local maxima of ELI-D in the valence shells (i.e., 4th shell) of the Fe1 and Fe2 atoms. Owing to the high, but unsymmetrical coordination of the Fe atoms (Figure 4a), there is no
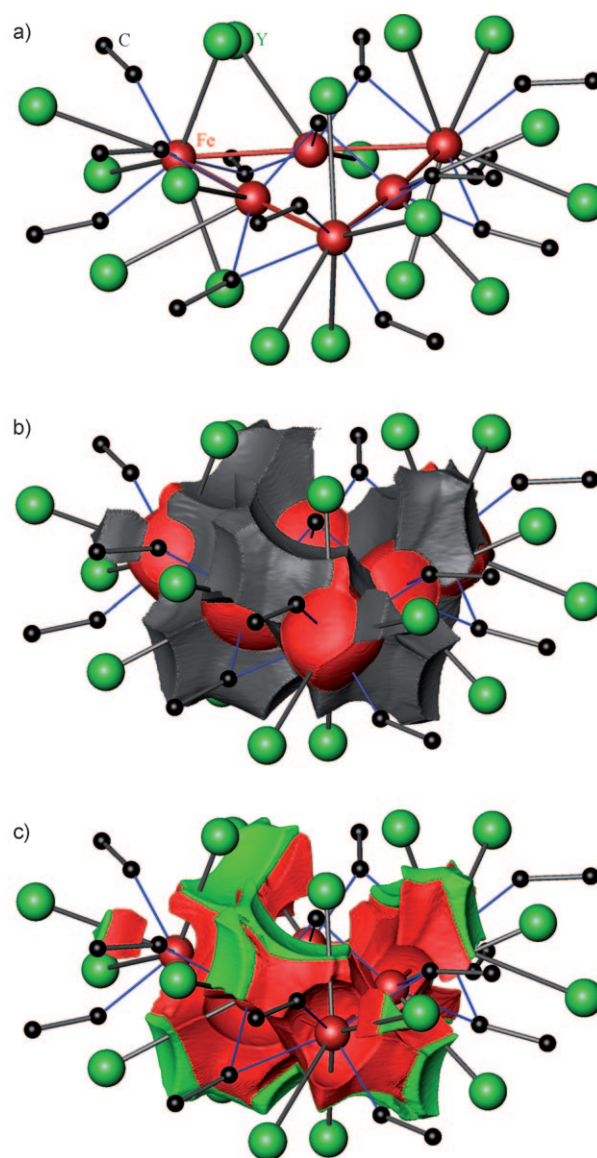


**Figure 4.** a) Nearest neighbors of the $Fe_6$ cluster, b) $Fe_6$ cluster superbasin of ELI-D (gray) and Fe 3rd shell basins (red), and c) $Fe_6$ cluster superbasin of ELI-D intersected by QTAIM atoms for $Y_{15}Fe_8C_{25}$. Red: Fe, green: Y atoms.

clear-cut distinction between intracluster and external bonding basins. As a characteristic, all of these basins possess attractors located inside the Fe atomic basins of the electron density, i.e., within the QTAIM Fe1 and Fe2 atoms. As an adequate procedure, all of these $Fe_6$ cluster ELI-D basins were united into one cluster superbasin, a general procedure proposed by Silvi.[25] The lone-pair-type basins of the carbon ligands establishing dative bonds to the Fe atoms are clearly separated from the cluster superbasin. The $Fe_6$ cluster superbasin is depicted in gray in Figure 4b. The separated Fe 3rd shell ELI-D basins marked in red are completely located inside the corresponding QTAIM Fe atom and touch the cluster superbasin (Figure 4b). Integration of the electron density within the ELI-D cluster superbasin reveals a sizable electronic population of 8.2 e⁻. Integration of the spin density

within the ELI-D basins reveals only a small degree of spin polarization (0.1 e$^-$) within the cluster superbasin. As is to be expected, the highest spin polarization is found in the 3rd shell regions of the Fe atoms of the cluster (3.9 e$^-$ in total).

All these results give rise to the notion of a covalently bonded, magnetic Fe$_6$ cluster stabilized by dative ligand-to-metal bonds. However, this is not yet the complete picture. Recent investigations of novel organometallic complexes with unsupported RE–T bonds, for example, Cp$_2$Y–ReCp$_2$,[26a] La(−ReCp$_2$)$_3$,[26b] and exemplary analysis of RE–T interactions in La$_7$Os$_4$C$_9$,[21] revealed the presence of polar covalent RE–T interactions. The picture is that of a dative bond between an electron-rich T atom and a coordinatively unsaturated RE metal involving a T "lone pair" created by the specific arrangement of strongly interacting electron-donor ligands.

The present case can be considered an extension of this picture. The Fe atoms are rather electron-rich with effective QTAIM charges of −0.1 and +0.2 for Fe1 and Fe2 cluster atoms, respectively. They are not only strongly interacting with the carbon ligands but also among each other, which gives rise to a sizable number of electrons (1.37 e$^-$ per cluster Fe atom) in the valence region of the 3d transition metal. The formation of electron localizability maxima in the valence region of a T element forming a pure d–d covalent interaction in a T$_2$ dimer has been already exemplarily demonstrated.[27] Here, the Fe$_6$ cluster superbasin also contains such regions. The whole superbasin serves as an electron-donor region for the attached RE atoms. The polarity of the interactions can be investigated applying the method of ELI-D/QTAIM basin intersection in analogy to the corresponding ELF/QTAIM intersection procedure.[28] The intersection of the ELI-D cluster superbasin with the QTAIM atomic basins of Fe and Y is shown in Figure 4c, with most of the volume of the superbasin belonging to the QTAIM Fe atoms (red color) and only a minor part (green color) to the Y atoms. Integration of the electron density in the intersection parts reveals that 7.2 e$^-$ (88 %) out of the total 8.2 e$^-$ belong to the Fe$_6$ cluster atoms and only 11 % to the attached Y atoms. The largest populations for the Y atom intersections are found above and below the Fe$_6$ cluster plane, corresponding to the shortest Fe–Y contacts (Fe1–Y3 = 274 pm). Although this distance is the same above and below the plane, the intersections are not. The reason is the missing monoatomic carbon ligand below the plane leading to more extended superbasin regions on the bond-opposed side and to twice as large populations of the intersecting Y regions. From this point of view, the only one-sided coordination of the Fe$_6$ cluster by monoatomic carbon enhances the Fe–Y bonding relative to two-sided coordination.

In summary, the crystal structures of the isotypic compounds RE$_{15}$Fe$_8$C$_{25}$ (RE = Y, Dy, Ho, Er) contain planar (magnetic) Fe$_6$ clusters characterized by covalent Fe–Fe bonding interactions. Besides one monoatomic carbon atom a total of 12 diatomic carbon ligands are attached to the clusters, thereby forming trigonal planar Fe(C$_2$)$_3$ units interconnecting the Fe$_6$ groups to a complex polymeric anion $_\infty^2$[(Fe$_6$)Fe$_2$(C$_2$)$_{12}$C]. The RE atoms surrounding the clusters along [001] reveal significant contributions to chemical

bonding Fe→RE in the sense of polar dative interactions. RE species are assigned a RE$^{3+}$ oxidation state. Fe atoms are present in low valence states with only small effective charges (QTAIM method) of −0.1 and +0.2 for the cluster atoms (Fe1, Fe2) and +0.15 for iron in trigonal planar coordination (Fe3). A rough estimation of the valence states of iron by simple electron counting leads to Fe(3)$^{1+}$ and Fe(1,2)$^{0.83+}$, which are significantly different from the effective charges, but reflect the general trend to low valence states. Besides our continuing Mössbauer investigations on the Fe$_6$ cluster compounds, further work is focused on the stabilization of even larger clusters in the systems REFeC.

[1] E. Dashjav, G. Kreiner, W. Schnelle, F. R. Wagner, R. Kniep, W. Jeitschko, *J. Solid State Chem.* **2007**, *180*, 636–653.

[2] M. H. Gerss, W. Jeitschko, L. Boonk, J. Nienstedt, J. Grobe, E. Mörsen, A. Leson, *J. Solid State Chem.* **1987**, *70*, 19–29.

[3] R.-D. Hoffmann, R. Pöttgen, W. Jeitschko, *J. Solid State Chem.* **1992**, *99*, 134–139.

[4] B. Rohrmoser, G. Eickerling, M. Presnitz, W. Scherer, V. Eyert, R-D. Hoffmann, U. Ch. Rodewald, C. Voigt, R. Pöttgen, *J. Am. Chem. Soc.* **2007**, *129*, 9356–9365.

[5] R. Pöttgen, W. Jeitschko, U. Wortmann, M. E. Danebrock, *J. Mater. Chem.* **1992**, *2*, 633–637.

[6] W. Jeitschko, M. H. Gerss, *J. Less-Common Met.* **1986**, *116*, 147.

[7] A. M. Witte, W. Jeitschko, *Z. Naturforsch. B* **1996**, *51*, 249–255.

[8] B. Davaasuren, E. Dashjav, G. Kreiner, H. Borrmann, M. Mihalkovic, R. Kniep, *J. Solid State Chem.* **2009**, *182*, 1331–1335.

[9] H. H. Stadelmeyer, H. K. Park, *Z. Metallkd.* **1982**, *73*, 399–402.

[10] H. K. Park, H. H. Stadelmeyer, L. T. Jordan, *Z. Metallkd.* **1981**, *72*, 417–422.

[11] Mixtures of the elements (RE: pieces, AMES, Fe: pieces, Alfa, and graphitic carbon: 99.95 %, Chempur) in the molar ratio 15:8:26 were pressed into pellets, arc-melted, and annealed at 1373 K in Ta ampoules jacketed in fused silica tubes for 500 h. All handlings were performed under Ar atmosphere. For further details, see the Supporting Information.

[12] XRPD (3° < 2θ < 100°, Huber Guinier camera 670, Co K$\alpha_1$-radiation, λ = 178.8965 pm, transmission geometry, Ge monochromator, flat sample holder with mylar foil). Refinement of the lattice parameters: LaB$_6$ as internal standard (SRM660a, a = 415.6916 pm); crystallographic data of Er$_{15}$Fe$_8$C$_{26}$: *P*321; *Z* = 6; a = 1186.02(2) pm, c = 508.85(1) pm; Rigaku RAXIS Spider, Ag$_{K\alpha}$ radiation; 295 K; 4.14 < θ < 44.5; structure solution by direct methods; crystal size: 0.02 × 0.01 × 0.01 mm$^3$; μ = 29.21 cm$^{-1}$; ρ = 8.722 g cm$^{-3}$; the crystal was twinned (twin law 010 100 001, twin fraction = 0.33; *R*1 = 0.02 and w*R*2 = 0.03 for all 6330 reflections and 78 variables. Further details on the crystal structure investigations may be obtained from the Fachinformationszentrum Karlsruhe, 76344 Eggenstein-Leopoldshafen, Germany (fax: (+49) 7247-808-666; e-mail: crysdata@fiz-karlsruhe.de), on quoting the depository number CSD-421364. See also the Supporting Information.

[13] *P*321; *Z* = 1; Y$_{15}$Fe$_8$C$_{25}$: a = 1194.92(4) pm, c = 513.83(3) pm; Dy$_{15}$Fe$_8$C$_{25}$: a = 1192.63(2), c = 514.36(2) pm, Ho$_{15}$Fe$_8$C$_{25}$: a = 1189.11(7) pm, c = 511.26(5) pm, Further details on the crystal structure investigation may be obtained from the Fachinformationszentrum Karlsruhe, 76344 Eggenstein-Leopoldshafen, Ger-

many (fax: (+ 49) 7247-808-666; e-mail: crysdata@fiz-karlsruhe. de), on quoting the depository numbers CSD-421364, CSD-420018, and CSD-421467).

[14] J. Häglund, F. F. Guillermet, G. Grimvall, M. Korling, *Phys. Rev. B* **1993**, *48*, 11685–11691.

[15] H. L. Yakel, *Int. Met. Rev.* **1985**, *30*, 17–40.

[16] Z. Q. Lv, S. H. Sun, P. Jiang, B. Z. Wang, W. T. Fu, *Comput. Mater. Sci.* **2008**, *42*, 692–697.

[17] M. H. Gerdes, W. Jeitschko, K. H. Wachtmann, M. E. Danebrock, *J. Mater. Chem.* **1997**, *7*, 2427–2431.

[18] a) G. Kresse, J. Furthmüller, *Phys. Rev. B* **1996**, *54*, 11169–11186; b) G. Kresse, J. Joubert, *Phys. Rev. B* **1999**, *59*, 1758–1775.

[19] O. Jepsen, A. Burkhard, O. K. Andersen, The Program TB-LMTO-ASA, version 4.7, Max-Planck-Institut für Festkörperforschung, Stuttgart, Germany, **1999**.

[20] U. Barth, L. Hedin, *J. Phys. C* **1972**, *5*, 1629–1642.

[21] E. Dashjav, Yu. Prots, G. Kreiner, W. Schnelle, F. R. Wagner, R. Kniep, *J. Solid State Chem.* **2008**, *181*, 3121–3130.

[22] R. Dronskowski, P. E. Blöchl, *J. Phys. Chem.* **1993**, *97*, 8617–8624.

[23] a) M. Kohout, *Int. J. Quantum Chem.* **2004**, *97*, 651–658; b) M. Kohout, K. Pernal, F. R. Wagner, Yu. Grin, *Theor. Chem. Acc.* **2004**, *112*, 453–459; c) M. Kohout, *Faraday Discuss.* **2007**, *135*, 43–54; d) M. Kohout, F. R. Wagner, Yu. Grin, *Theor. Chem. Acc.* **2008**, *119*, 413–420.

[24] R. F. W. Bader, *Atoms in Molecules: A Quantum Theory*, Oxford University Press, Oxford, **1994**.

[25] B. Silvi, *J. Mol. Struct.* **2002**, *614*, 3–10.

[26] a) M. V. Butovskii, O. L. Tok, F. R. Wagner, R. Kempe, *Angew. Chem.* **2008**, *120*, 6569–6572; *Angew. Chem. Int. Ed.* **2008**, *47*, 6469–6472; b) M. V. Butovskii, C. Döring, V. Bezugly, F. R. Wagner, Yu. Grin, R. Kempe, *Nat. Chem.* **2010**, DOI: 10.1038/nchem.718.

[27] M. Kohout, F. R. Wagner, Yu. Grin, *Theor. Chem. Acc.* **2002**, *108*, 150–156.

[28] G. Jansen, M. Schubart, B. Findeis, L. H. Gade, I. J. Scowen, M. McPartlin, *J. Am. Chem. Soc.* **1998**, *120*, 7239–7251.